Journal of Manufacturing Processes 102 (2023) 874–884

Contents lists available at ScienceDirect

Journal of Manufacturing Processes

journal homepage: www.elsevier.com/locate/manpro

Chatter reliability of high speed cylindrical grinding with uncertain parameters

Wei Feng [a], Peng Qin [a,*], Le Cao [a], Cong Sun [b], Wei Li [c], Xiaojun Cao [a]

[a] Henan Key Laboratory of Super Hard Abrasives and Grinding Equipment, Henan University of Technology, Zhengzhou 450001, China
[b] Northeastern University, Shenyang 110819, China
[c] Hunan University, Changsha 410082, China

ARTICLE INFO

Keywords:
Cylindrical grinding
Grinding chatter
Reliability analysis

ABSTRACT

Cylindrical grinding is commonly used as the final process of machining, but its quality and efficiency are often limited by chatter phenomenon. Many research show that the result from conventional chatter analysis by using the deterministic parameters is not consistent with the practical working condition and the chatter reliability prediction in high speed cylindrical grinding with uncertain parameters is studied in this paper. The dynamic model of the cylindrical grinding system is established, and uncertain parameters such as mass, stiffness and damping coefficient are introduced, and the stability lobe diagrams with uncertain parameters were obtained. The reliability model of the grinding system was established, and the reliability was solved by using the Monte Carlo simulation method, the improved first-order second-moment method and the second-order second-moment method, respectively. Then, the chatter-free reliability of the system was predicted by using the reliability lobe diagram. The accuracy of the grinding reliability prediction results is verified by the experiment results. Furthermore, the Monte Carlo sensitivity analysis method is used to study the influence of random parameters on the grinding system, and the results show that the variation of modal mass has the greatest influence on the reliability of the grinding system.

1. Introduction

Grinding is usually used as the final process of machining, which directly affects the machining accuracy and surface quality of workpiece. In recent years, high speed precision grinding technology has been widely used in many fields such as aerospace, automobile industry, metallurgy and national defense industry, etc. With the improving requirements on grinding precision and high speed of grinding wheel [1,2], higher requirements of the grinding process stability are required.

Due to the emerging tendency on the grinding chatter research, many research have been proposed [3–6]. Hahn [7] introduced regenerative chatter theory to grinding chatter and the regeneration phenomenon of the workpiece surface during the grinding process is studied. Snoeys and Brown [8] considered the regeneration chatter theory of workpiece and grinding wheel at the same time. Combined with the Nyquist diagram, the chatter in the grinding process is analyzed. Altintas and Weck [9] established the kinematic model of longitudinal cylindrical grinding and discussed the chatter phenomenon through numerical simulation. Li and Shin [10] proposed a time-domain simulation method to predict the chatter boundary conditions and chatter growth rates of the cylindrical grinding system, which taking the geometric interference between the grinding wheel and the workpiece into consideration. Liu and Payre [11] studied the stability of the cylindrical grinding by calculating the frequency spectrum of the double delay differential. Kim et al. [12] established a dynamic model considering the double regeneration phenomenon of the workpiece and the grinding wheel. By building and analyzing the four-degree-of-freedom dynamic model of plunge grinding, Yan et al. [13] obtained the grinding stability diagram and used it to determine the stability boundary of regenerative chatter and friction chatter. With the use of the receptance coupling substructure analysis (RCSA), Leonesio et al. [14] established a frequency-domain characterization to show the interaction between the machine tool and the cylindrical grinding process, and used it for grinding stability analysis. Chen et al. [15] studied the influence of grinding chatter and grinding wheel eccentricity on the dynamic performance of surface grinding, and made qualitative and quantitative studies on the grinding stability under the variable grinding force and grinding wheel eccentricity. Tóth et al. [16] studied an alternative

* Corresponding author.
E-mail address: peng_qin@haut.edu.cn (P. Qin).

https://doi.org/10.1016/j.jmapro.2023.08.012
Received 25 June 2023; Received in revised form 1 August 2023; Accepted 8 August 2023
Available online 7 September 2023

grinding wheel regeneration effect for distributed abrasive passivation and predicted the stability for the one-stroke surface grinding.

In recent years, the reliability of machining stability has attracted the attention of many scholars and a lot of research have been carried out [17]. In practical condition, parameters will show certain uncertainties, like structural modal parameters and material performance parameters, etc. These uncertain factors will lead to uncertainties in parameters such as mass, stiffness and damping in the dynamic model, which leading to affect the chatter prediction results. Duncan et al. [18] studied the influence of random parameters on the stability lobe diagram (SLD), and obtained three different SLDs by using the parameters of the mean value and the value from mean plus or minus standard deviation. Considering the model parameters as random variables, Totis et al. [19,20] analyzed the stability of the uncertain dynamic milling model, and obtained the probabilistic SLD. They also proposed three new probabilistic analytical method, based on the polynomial chaos and Kriging proxy model. Zhang et al. [21] designed a spindle speed optimization method for parameter uncertainties and the lower boundary of the SLD was used as an optimization constraint. Considering the uncertainty of the natural frequency of the machining system and the cutting force coefficient, Graham et al. [22] proposed a robust stability model for milling, which has a higher prediction reliability compared with traditional methods. Considering the influence of the randomness of parameters on the turning stability, Huang et al. [23] used the Monte Carlo simulation method and the improved first-order second-order moment method to predict the reliability of the turning stability. Considering the structural parameters mass, stiffness, damping and the spindle speed as random parameters, Liu et al. [24] used the reliability lobe diagram (RLD) to judge the chatter and non-chatter regions. As for the chatter in the milling process, Löser et al. [25] proposed an effective calculation method for the confidence level of the milling stability region in the frequency domain, based on the dynamic grinding force and the dynamic grinding process. Considering the uncertainty in the frequency response function (FRF) of the tool tip, Hajdu et al. [26,27] obtained the reliable stability region of the machining system with uncertain parameters by using pseudo-spectrum method and stability boundary. Then, as for the milling system with modal uncertainties, they used the same method to obtain the stable region of system reliability with uncertain modal parameters. Li et al. [28] proposed a novel method to determine the milling stability boundary. The most influential parameters were determined through sensitivity analysis and the Bayesian inference method was constructed to calculate the milling stability. Ahmadi [29] proposed an updated Bayesian method for process calibration of chatter model parameters in turning operation, and conducted experiments to verify the efficiency and effectiveness of the method in improving the accuracy of turning chatter prediction. However, there are few research on the chatter reliability of grinding. Sun et al. [30] proposed a model combining non-Gaussian distribution of abrasive particles and grinding chatter. By using the Monte Carlo method and the first-order second-order moment method, the relationship between grinding parameters such as wheel speed, feed speed, abrasive particle size and workpiece surface quality were studied.

The remainder of this paper is organized as follows. Section 2 briefly presents the calculation of the stability of cylindrical grinding. Section 3 presents the dynamic modeling of the grinding system considering the uncertainty of dynamic parameters m, c, k and frequency ω. Section 4 presents three different chatter reliability analysis methods and proposed an updated improved first-order second-order moment method. The sensitivity of each random parameter on the stability of the dynamic grinding system are analyzed in Section 5 and they are verified by grinding experiment shown in Section 6. Finally, the conclusions are drawn in Section 7.

2. Dynamic modeling of cylindrical grinding

The regenerative chatter system of the external cylindrical plunge grinding process can be simplified as a single-degree-of-freedom model, as shown in Fig. 1. Based on the results of impact tests and grinding experiment, the workpiece is considered to have good rigidity. The radial direction of the grinding wheel with larger force and vibration are considered for dynamic analysis. Considering that the fundamental frequency contributes the most, only the first mode is considered in this research. By knowing that the elastic force is proportional to the vibration displacement and the damping force is proportional to the first derivative of the vibration displacement, the dynamic equation of the grinding system can be obtained as

$$m\ddot{X}(t) + c\dot{X}(t) + kX(t) = F(t) \tag{1}$$

where,m—the modal mass of the grinding system, kg;c—the modal damping of the grinding system, N s/m;k—the modal stiffness of the grinding system, N/m;$X(t)$—the vibration displacement of the grinding wheel at time t in the radial direction, m;$F(t)$—the dynamic grinding force at time t, N.

Considering that the dynamic grinding force is proportional to the material removal rate, it can be expressed as

$$F(t) = k_m hba(t) \tag{2}$$

$$a(t) = a_0 - [X(t) - X(t-T)] \tag{3}$$

where,k_m—the grinding force coefficient, N/m^3;h—the grinding depth, m;b—the contact width in the cylindrical grinding, m;$a(t)$—the surface vibration of the grinding wheel, m;a_0—the initial surface vibration of the grinding wheel, m;T—the rotation period of the grinding system, s.

Substituting Eqs. (2) and (3) into Eq. (1), and conducting the Laplace transform, Eq. (4) can be obtained as follow.

$$\left(ms^2 + cs + k\right)X(s) = k_m hb\left[a_0(s) - X(s) + e^{-Ts}X(s)\right] \tag{4}$$

Then, the transfer function of regenerative chatter system in the cylindrical grinding can be expressed as Eq. (5).

$$G(s) = \frac{X(s)}{a_0(s)} = \frac{k_m hb\frac{1}{k}W(s)}{1 + (1 - e^{-sT})k_m hb\frac{1}{k}W(s)} \tag{5}$$

where $W(s)$ is the dynamic characteristic of grinding system, which can be expressed as Eq. (6).

$$W(s) = \frac{1}{\frac{s^2}{\omega_n^2} + \frac{2\xi}{\omega_n}s + 1} \tag{6}$$

where ω_n is natural frequency which expressed as $\omega_n = \sqrt{k/m}$ and ξ is the damping ratio which expressed as $\xi = c/\left(2\sqrt{mk}\right)$.

Let the denominator in Eq. (6) be zero, and the characteristic

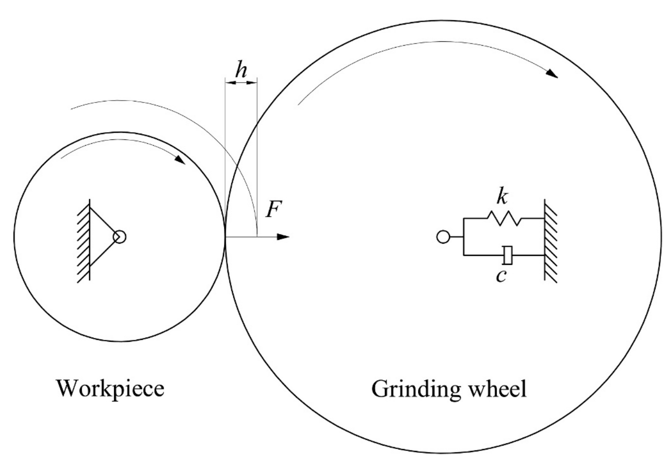

Fig. 1. Modeling of cylindrical plunge grinding system.

equation of the chatter system can be obtained as Eq. (7).

$$1+\left(1-e^{-sT}\right)k_m hb\frac{W(s)}{k}=0 \tag{7}$$

Eq. (7) is the regenerative chatter condition of the grinding system. According to the stability determination theory, when the characteristic root is $s=j\omega$, the system is in a critical stable condition. By substituting $s=j\omega$ into Eq. (7), the following Eq. (8) can be obtained.

$$\frac{W(j\omega)}{k}=-\frac{1}{k_m hb\left(1-e^{-j\omega T}\right)} \tag{8}$$

where ω is angular frequency.

By using Harmonic Balance Method, Eq. (9) can be obtained from Eq. (8).

$$\omega T=2i\pi+arcsin\frac{2\xi\lambda}{\sqrt{(2\xi\lambda)^2+\left(1-\lambda^2\right)^2}}-arctan\frac{2\xi\lambda}{1-\lambda^2}(i=1,2,\cdots,m) \tag{9}$$

where λ is the frequency ratio which can be expressed as $\lambda=\omega/\omega_n$.

Then, the relationship between the spindle speed and critical grinding depth can be expressed as Eqs. (10) and (11)

$$n=\frac{60\lambda\omega_n}{\omega T} \tag{10}$$

$$h_{\lim}=\frac{2\xi\lambda k}{k_m bsin(\omega T)} \tag{11}$$

Through the theoretical analysis and derivation process above, the critical grinding depth $h_{\lim}$ at the certain speed can be obtained which means that the SLD can be plotted. The relationship between dynamic parameters *m*, *c*, *k*, grinding force coefficient k_m and chatter angular frequency ω and the critical grinding depth $h_{\lim}$ can also be obtained. Instead of using the time domain method to get the SLD, the method proposed above is a kind of frequency domain method which has high computational efficiency but low accuracy. Considering that the chatter reliability prediction is focused in this paper and the SLD is used to make a comparison than make a decision in practical machining, the proposed method will be used in the following part.

3. Dynamic modeling with uncertain parameters

In the calculation of the critical grinding depth, the dynamic parameters *m*, *c*, *k* and frequency ω are conventionally regarded as fixed parameters. However, these parameters are not constant in practical machining process, considering the assembly errors, machining errors, measurement errors, and environmental factors, etc. Therefore, it is necessary to quantitatively analyze the uncertainty and the statistical method and stochastic mathematical method are the parametric uncertainty quantization methods that be often used. Among them, the Monte Carlo method is a numerical calculation method based on random sampling, which has the advantages of simple operation, high flexibility and wide application range. In the analysis and research, the results of Monte Carlo method are usually taken as the reference.

Considering the uncertainty of *m*, *c* and *k*, they are regarded as random variables and be introduced into Eq.(1) to get the uncertain dynamic model as expressed in Eq.(12).

$$m_R\ddot{X}(t)+c_R\dot{X}(t)+k_RX(t)=F(t) \tag{12}$$

where,m_R is the modal mass of the grinding system under R-times sampling, kg;c_R is the modal damping of grinding system under R-times sampling, N s/m;k_R is the modal stiffness of the grinding system under R-times sampling, N/m.

In order to get the statistical distribution of *m*, *c*, and *k*, a series of impact tests were conducted on a high-precision CNC grinding machine with model number CNC8325, as shown in Fig. 2a). A force hammer with model number PCB086C03 was used for the single point excitation in both horizontal and vertical directions of grinding wheel. An acceleration sensor with model number 352C03 is installed at the grinding wheel center to collect response signals. The FRF of the system can be obtained by analyzing the collected signals from both force hammer and acceleration sensor, as shown in Fig. 2b). The impact tests were carried out several times to obtain 20 sample values, and the mean values and standard deviations of the system dynamic parameters were obtained and shown in Table 1.

The grinding force coefficient is obtained from reference [31] which is $k_{\mathrm{m}}=2.7\times10^{12}$ N/m^3, and the SLD can be calculated by using Eqs. (10) and (11). Using the Monte Carlo method to sample 10 times, the SLDs with random parameters can be plotted as shown in Fig. 3. It can be seen that all the SLDs are accumulated in a certain area and the stable grinding depth will change as the parameters change. Therefore, there will be some errors in the stability prediction results when using deterministic parameters.

From Eqs. (10) and (11), it can be observed that the critical grinding depth is related to the dynamic parameters *m*, *c*, *k* and chatter frequency ω. In the high speed cylindrical grinding, *m*, *c*, *k* can be considered as independent random parameters, and the chatter frequency ω is a variable determined by them. In order to analyze the reliability of the grinding system, it is necessary to obtain the distribution parameter estimation of chatter frequency ω and it can be expressed as Eq. (13) considering the critical grinding equations.

Table 1
Mean and standard deviation of dynamics parameters.

Dynamics parameters	Mass, *m* (kg)	Damping, *c* (N·s/m)	Stiffness, *k* (N/m)
Mean	24.9	521	3.07×10^6
Standard deviation	0.1	30	10^5

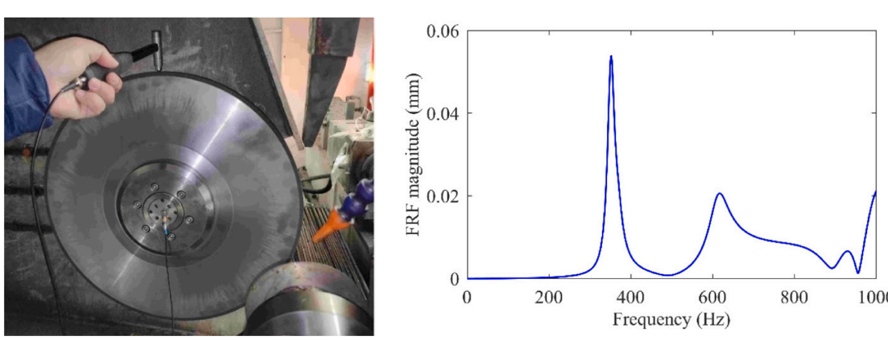

a) Photo of impact test b) Obtained FRF

Fig. 2. Impact test and FRF of grinding system.

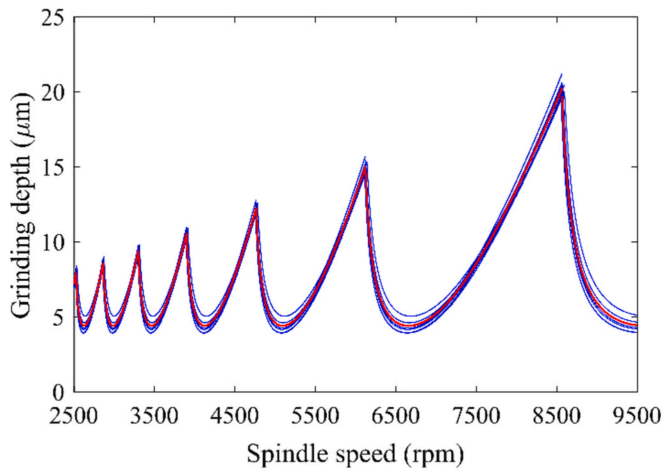

Fig. 3. Stability lobe diagram with random parameters.

$$\omega = f(m, c, k, \Omega) \tag{13}$$

Assuming that the dynamic parameters m, c and k in grinding system meet the normal distribution. The critical grinding depth and chatter frequency can be calculated by sampling the dynamic parameters m, c, k. The spindle speeds at 4000 rpm, 5000 rpm, 5500 rpm and 6000 rpm are selected and 5000 samples are conducted. The obtained chatter frequencies at different spindle speeds are shown in Fig. 4. The means and standard deviations of each chatter frequency are ω_1 (985.1841, 2.8495), ω_2 (1099.9155, 2.0259), ω_3 (985.1841, 2.8495) and ω_4 (1099.9155, 2.0259), respectively.

The calculated chatter frequency samples were tested for goodness of fit. Under the condition of a significance level of 5 %, all the chatter frequencies are verified to meet the normal distribution.

4. Grinding chatter reliability analysis

Grinding chatter reliability refers to the ability to work in accordance with the expected function and performance under certain conditions, specifically, it can be regarded as the probability that the system functions and performance meet the expectations stably within a certain period of time. There are two kinds of mechanical reliability analysis methods that commonly used, namely the Monte Carlo simulation method and the moment method. The Monte Carlo method is used to solve the reliability by substituting random parameters with a certain probability distribution into the model to simulate the random phenomena in the grinding process. The moment method mainly includes the first order second moment method (FOSM), the improved first order second moment method, the second order second moment method (SOSM) and the fourth order moment method. The FOSM is used to calculate the failure probability by linearly approximating the critical state surface on the failure surface. On the basis of the FOSM, by considering the curvature of the surface in the critical state, the SOSM is used to correct the results of the first analysis twice, which improves the calculation accuracy. The Monte Carlo simulation method (MCS) has the characteristics of high accuracy but long time, and the calculation efficiency is higher than the moment method.

4.1. Modeling of grinding chatter reliability

When using the the critical grinding depth of the SLD obtained from certain parameters, the grinding chatter may occur. Therefore, it is necessary to analyze the reliability of SLD. The critical state function of the grinding reliability can be expressed as Eq. (14).

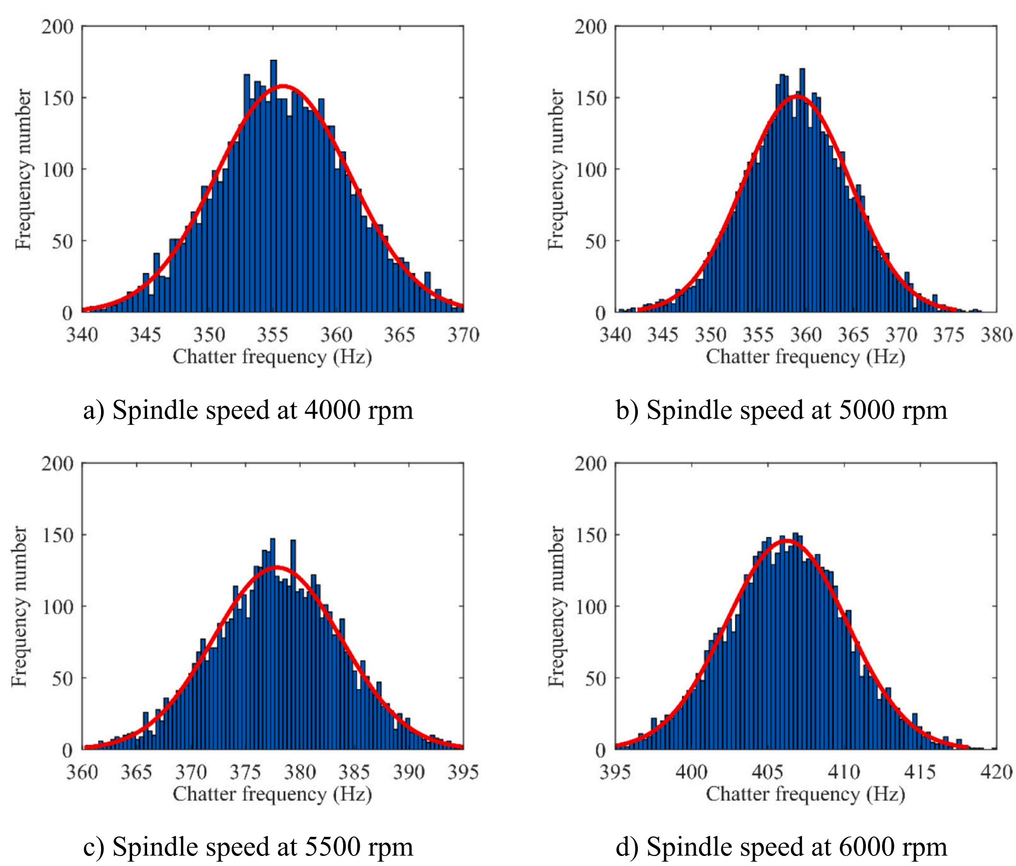

Fig. 4. Histogram of chatter frequency distribution at different spindle speeds.

$$g_x(X) = h_{\lim} - h_0 \tag{14}$$

where,h_0 is a given grinding depth which can be regarded as a threshold value, m;X is the random variable of the grinding system parameters, which can be expressed as $X = [m\ c\ k\ \omega]^T$.

The reliability of the grinding system can be defined as the probability that the critical grinding depth over the given grinding depth, which can be expressed as Eq. (15).

$$\begin{cases} g_X(X) = h_{\lim} - h_0 \geq 0 \\ h_{\lim} = f(m, c, k, \omega) \end{cases} \tag{15}$$

4.2. Reliability calculation with the improved FOSM

By knowing that the random parameters meet the normal distribution, the nonlinear functional function is selected from the point of maximum failure probability contribution. After linearization with the Taylor's expansion, the first-order moment and second-order moment of the functional function are obtained, and the reliability of the system is also obtained approximately.

The equation of the critical cylindrical grinding system can be expressed as

$$Z = g_x(X) = 0 \tag{16}$$

All the random parameters m, c, k and ω meet the normal distribution. Among them, m, c, k are random parameters that are independence to each other and they are all related to the chatter frequency ω. Random parameters need to be orthogonalized and transformed into linearly independent random parameters. The linearly dependent random parameter is transformed into a linearly independent random parameter by using the orthogonal transformation method. The covariance matrix C of the grinding system can be expressed as Eq. (17).

$$C = \begin{Bmatrix} \sigma_1^2 & 0 & 0 & \rho_{X_1X_4}\sigma_1\sigma_4 \\ 0 & \sigma_2^2 & 0 & \rho_{X_2X_4}\sigma_2\sigma_4 \\ 0 & 0 & \sigma_3^2 & \rho_{X_3X_4}\sigma_3\sigma_4 \\ \rho_{X_4X_1}\sigma_1\sigma_4 & \rho_{X_4X_2}\sigma_1\sigma_4 & \rho_{X_4X_3}\sigma_1\sigma_4 & \sigma_4^2 \end{Bmatrix} \tag{17}$$

where σ_1, σ_2, σ_3, and σ_4 are the standard deviations of random parameters m, c, k and ω respectively. ρ is the correlation coefficients of random parameters.

Let the vector quantity A be the eigenvector which can make matrix C convert to a diagonal matrix. Conduct an orthogonal transformation and make vector X transform into a linearly independent vector Y, which can be expressed as Eqs. (18) and (19).

Let the vector quantity A be the eigenvector which can make matrix C convert to a diagonal matrix. Conduct an orthogonal transformation and make vector X transform into a linearly independent vector Y, which can be expressed as Eqs. (18) and (19).

$$X = AY \tag{18}$$

$$Y = A^T X \tag{19}$$

After transformation, the mean and variance of vector Y are expressed as Eqs. (20) and (21).

$$\mu_Y = A^T \mu_X \tag{20}$$

$$D_Y = A^T CA \tag{21}$$

The functional function expressed with linearly independent random parameters is shown as Eq. (22).

$$Z = g_x(X) = g_x(AY) = g_Y(Y) \tag{22}$$

Using the checking point method to solve the reliability of the grinding system, it is necessary to derive the random parameter Y, which can be expressed as Eq. (23).

$$\nabla g_Y(y^*) = A^T \nabla g_X(x^*) \tag{23}$$

The critical state eq. $Z = 0$ can be regarded as the tangent plane of the critical state through Y^*. Then, the mean and variance of vector Z_L can be expressed as Eqs. (24) and (25).

$$\mu_{Z_L} = g(Y^*) + \sum \frac{\partial g(Y^*)}{\partial Y_i}\left(\mu_{Y_i} - Y_i^*\right) \tag{24}$$

$$\sigma_{Z_L} = \sqrt{\sum_{i=1}^{4}\left[\frac{\partial g(Y^*)}{\partial Y_i}\right]\sigma_{Y_i}^2} \tag{25}$$

With the Eqs. (24) and (25), the reliable indicator for grinding system can be obtained as Eq. (26).

$$\beta = \frac{\mu_{Z_L}}{\sigma_{Z_L}} \tag{26}$$

The sensitivity coefficient of Y_i can be expressed as Eq. (27).

$$cos\theta_{Y_i} = -\frac{\frac{\partial g(Y^*)}{\partial Y_i}\sigma_{Y_i}}{\sqrt{\sum_{i=1}^{4}\left[\frac{\partial g(Y^*)}{\partial Y_i}\sigma_{Y_i}\right]^2}} \tag{27}$$

Let the coordinates of the checking point in the orthogonalized state random parameter Y space be Eq. (28).

$$Y^* = \mu_{Y_i} + \beta\sigma_{Y_i} cos\theta_{Y_i} \tag{28}$$

The coordinate of the original X space is obtained as Eq. (29).

$$X^* = AY^* \tag{29}$$

Conduct multiple iterative calculations on X until the difference between two adjacent time is within the allowable range, the reliability of the system is obtained as Eq. (30).

$$P_r = \varphi(-\beta) \tag{30}$$

The above is the procedure for solving the reliability using the improved FOSM, and its flow chart is shown in Fig. 5. In the calculation process, there is an update of the improved FOSM. In the common calculation, the correlation coefficient between two random variables is used to solve the covariance matrix. The correlation coefficient of random parameters used to be solved through sampling calculation, among which the random sampling data is small, the calculation results are inaccurate and the process is complicated. In order to solve these problems, the MCS is integrated into the improved FOSM. It is adopted to sample and to solve the covariance matrix directly, which makes it more convenience and accuracy.

4.3. Reliability calculation with the second order and second moments method

In this part, another method to solve the grinding reliability is proposed by using the Laplace asymptotic method and the SOSM. Knowing that the random parameters meet the normal distribution, the random parameters can be transformed into standard independent normal random parameters $Y = (Y_1, Y_2, \ldots, Y_n)^T$. Let the functional function be $Z = G_Y(Y)$, the failure probability of the grinding system can be expressed as Eq. (31).

$$P_f = \int_{gY(y)\leq 0} \varphi_n(y)dy = \int_{gY(y)\leq 0} \frac{1}{(2\pi)^{n/2}} exp\left(-\frac{y^T y}{2}\right)dy \tag{31}$$

The value of Eq. (31) is calculated by the Laplace integral, and its expression is shown as Eq. (32).

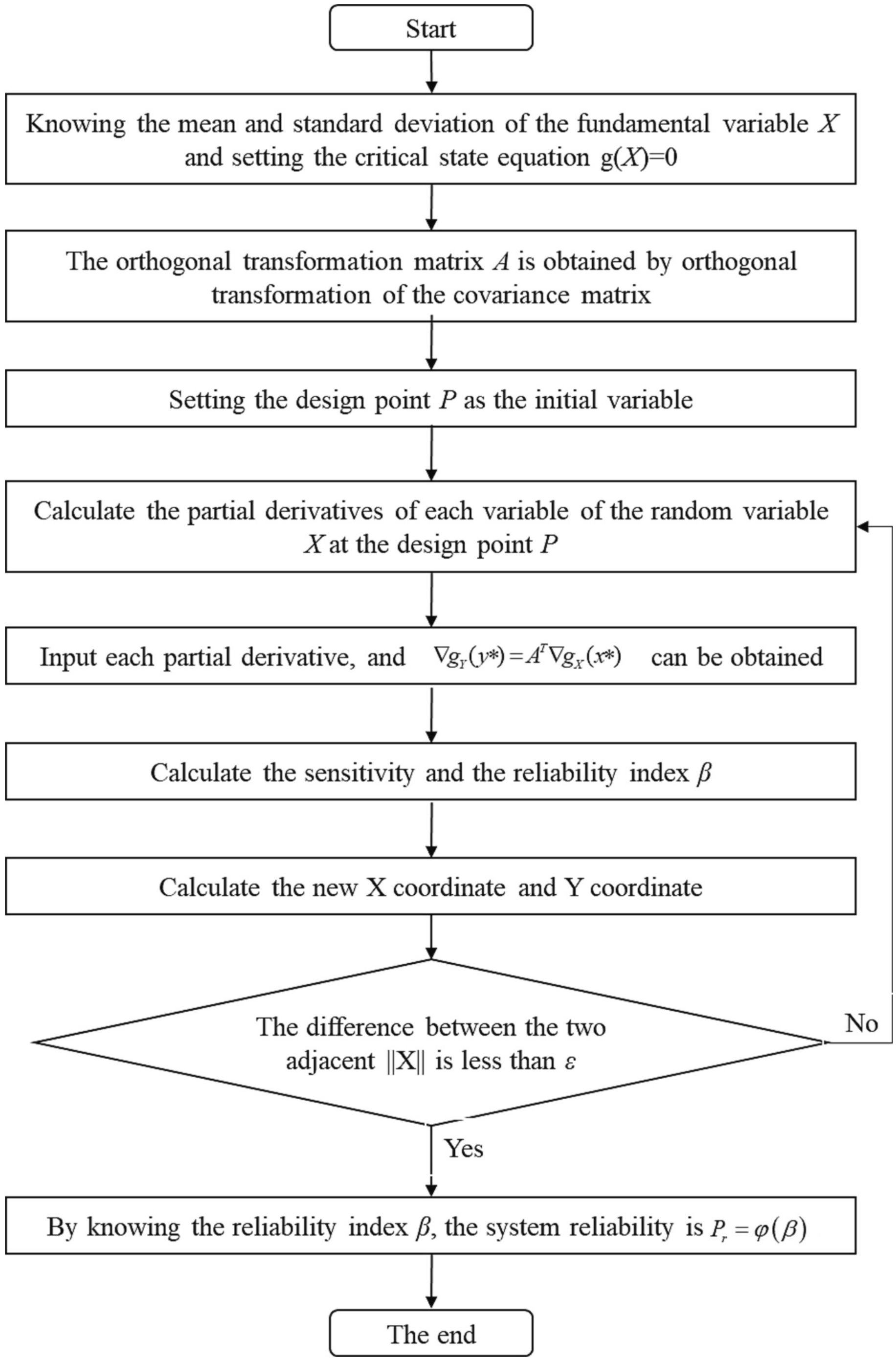

Fig. 5. Grinding system reliability using the improved FOSM.

$$I(\lambda) = \int_{g(x)\le 0} p(x)exp\left[\lambda^2 h(x)\right]dx \tag{32}$$

Considering that $h(x)$ takes the maximum value at a point x^* on the boundary$\{x|g(x)=0\}$of the integral domain, the integral value of Eq. (32) can be expressed as Eq. (33)

$$I(\lambda) \approx \frac{(2\pi)^{(n-1)}}{\lambda^{n+1}}\frac{p(x^*)exp\left[\lambda^2 h(x^*)\right]}{\sqrt{|J|}} \tag{33}$$

where

$$J = [\nabla h(x^*)]^T B(x^*)\nabla h(x^*) \tag{34}$$

Where the matrix $B(x^*)$ is the adjoint matrix $C(x^*)$ which shown in Eq. (35).

$$C(x^*) = \nabla^2 h(x^*) - \frac{\|\nabla h(x^*)\|}{\|\nabla g(x^*)\|}\nabla^2 g(x^*) \tag{35}$$

By choosing a large parameter $\lambda(\lambda \to +\infty)$, the transformation shown in Eq. (36) can be used.

$$Y = \lambda V \tag{36}$$

By substituting Eq. (36) into Eq. (31), Eq. (37) can be obtained.

$$P_f = \int_{g_Y(\lambda v) \le 0} \frac{\lambda^n}{(2\pi)^{n/2}} exp\left(-\frac{\lambda^2 v^T v}{2}\right) dv \tag{37}$$

Assuming that the functional function is differentiable quadratically, the asymptotic integral of Eq. (33) can be obtained as Eq. (38).

$$p = \frac{1}{\sqrt{2\pi}\lambda\sqrt{|J_1|}} exp\left(-\frac{\lambda^2 v^{*T} v^*}{2}\right) \tag{38}$$

where

$$J_1 = [\nabla h(v^*)]^T B(v^*) \nabla h(v^*) = v^{*T} B_1(v^*) v^* = \frac{1}{\lambda^2} y^{*T} B_1(v^*) y^* \tag{39}$$

The adjoint matrix of $C_1(v^*)$ is $B_1(v^*)$ and $C_1(v^*)$ be expressed as Eq. (40).

$$C_1(v^*) = \nabla^2 h(v^*) - \frac{\|\nabla h(v^*)\|}{\|\nabla g_Y(\lambda v^*)\|} \nabla^2 g_Y(\lambda v^*) \tag{40}$$

By substituting Eq. (39) into Eq. (38) and taking $\beta^2 = y^{*T} y^*$ into consideration, Eq. (41) can be obtained,

$$p = \frac{1}{\sqrt{2\pi}\sqrt{|J|}} exp\left(-\frac{y^{*T} y^*}{2}\right) = \frac{\varphi(\beta)}{\sqrt{|J|}} \tag{41}$$

where

$$J = y^{*T} B(y^*) y^* \tag{42}$$

$B(y^*) = B_1(v^*)$ is the adjoint matrix of $C(y^*) = C_1(v^*)$ shown in Eq. (27) and $C(y^*)$ can be expressed as Eq. (43).

$$C(y^*) = -I - \frac{\frac{1}{\lambda}\|y^*\|}{\lambda\|\nabla g_Y(y^*)\|} \lambda^2 \nabla^2 g_Y(y^*) = -I - \frac{\beta}{\|\nabla g_Y(y^*)\|} \nabla^2 g_Y(y^*) \tag{43}$$

Considering that the actual processing process β is generally a large positive value, $\varphi(\beta) \approx \beta\phi(-\beta)$ can be obtained and Eq. (41) can finally be approximated as Eq. (44).

$$p \approx \phi(-\beta) \frac{\beta}{\sqrt{|J|}} \tag{44}$$

Based on the SOSM, the grinding reliability calculation method with the Laplace asymptotic method under independent normal random parameters is proposed and its flow chart is shown in Fig. 6.

4.4. Analysis results comparison

The chatter reliability diagram can predict the chatter-free reliability

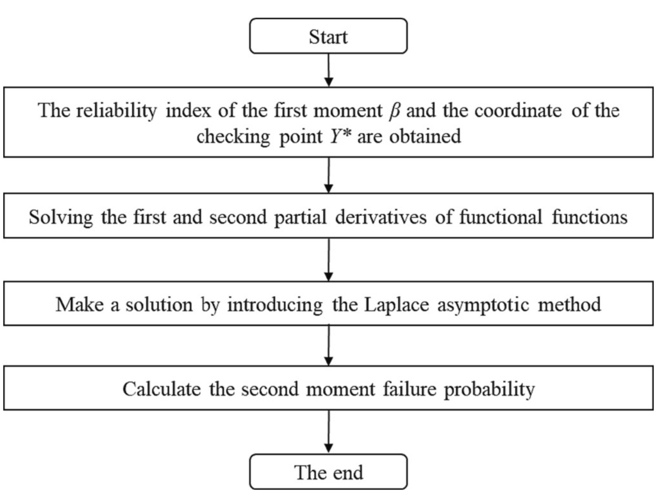

Fig. 6. Grinding system reliability using the SOSM.

of the grinding system with random characteristics. Except for judging whether chatter occurs in the grinding system, it can also reflect the stability level of the grinding system. The spindle speeds of 4000 rpm, 5000 rpm, 5500 rpm and 6000 rpm are selected and their reliability results are calculated by using the above two methods and the MCS for better comparison, as shown in Fig. 7. It can be observed that the reliability results solved by the improved FOSM and SOSM at four different spindle speeds are very close to the reliability values solved by the MCS.

5. Sensitivity analysis

In order to study the influence of each random parameter on the stability of the dynamic grinding system, the sensitivity analysis of grinding chatter is conducted. The influence of the above parameters on the vibration amplitude of the grinding system can be regarded as the influence on the stability of the cylindrical grinding system. In Eq. (14), let the means of the random parameters be $\mu_X = [\mu_m\ \mu_c\ \mu_k\ \mu_\omega]$ and the variances be $\sigma_X = [\sigma_m\ \sigma_c\ \sigma_k\ \sigma_\omega]$. The mean μ_Y and standard deviation σ_Y of the failure probability dynamic parameters m, c, k and chatter frequency ω can be solved by using the MCS. At the same time, the reliability sensitivity estimation of the correlation coefficient $\partial\rho_{Y_iY_j}$ can also be solved as expressed in Eqs. (45)–(47).

$$\frac{\partial\widehat{P}_f}{\partial\mu_{Y_i}} = \frac{1}{N}\frac{1}{\sigma_{Yi}}\sum_{k=1}^{N} I_F(y_k)\frac{y_{ki} - \mu_{Y_i}}{\sigma_{Y_i}} \tag{45}$$

$$\frac{\partial\widehat{P}_f}{\partial\mu_{Y_i}} = \frac{1}{N}\frac{1}{\sigma_{Yi}}\sum_{k=1}^{N} I_F(y_k)\left[\left(\frac{y_{ki} - \mu_{Y_i}}{\sigma_{Y_i}}\right)^2 - 1\right] \tag{46}$$

$$\frac{\partial\widehat{P}_f}{\partial\mu_{Y_iY_j}} = -\frac{1}{2N}\sum_{k=1}^{N} I_F(y_k)\left[(Y_{ki} - \mu_{Y_i})^T \frac{\partial C_y^{-1}}{\partial\rho_{Y_iY_j}}(Y_{ki} - \mu_{Y_i}) + \frac{1}{|C_y|}\frac{\partial|C_y|}{\partial\rho_{Y_iY_j}}\right] \tag{47}$$

where,

N is the number of samples;

$I_F(Y)$ is the indicator function when the sensitivity analysis index is $g(X) < 0$;

$\rho_{Y_iY_j}$ is the correlation coefficient of variables i and j;

C_y is the covariance matrix under the y coordinate;

y_{ki} is the random parameter i of sampling k times.

Then, the partial derivative of the reliability to the mean of the random variable X under the Y coordinate can be obtained as Eq. (48).

$$\begin{cases} \frac{\partial P_f}{\partial\mu_{X_m}} = \frac{\partial P_f}{\partial\mu_{Y_m}}\frac{\partial\mu_{Y_m}}{\partial\mu_{X_m}} + \frac{\partial P_f}{\partial\mu_{Y_c}}\frac{\partial\mu_{Y_c}}{\partial\mu_{X_m}} + \frac{\partial P_f}{\partial\mu_{Y_k}}\frac{\partial\mu_{Y_k}}{\partial\mu_{X_m}} + \frac{\partial P_f}{\partial\mu_{Y_\omega}}\frac{\partial\mu_{Y_\omega}}{\partial\mu_{X_m}} \\ \frac{\partial P_f}{\partial\mu_{X_c}} = \frac{\partial P_f}{\partial\mu_{Y_m}}\frac{\partial\mu_{Y_m}}{\partial\mu_{X_c}} + \frac{\partial P_f}{\partial\mu_{Y_c}}\frac{\partial\mu_{Y_c}}{\partial\mu_{X_c}} + \frac{\partial P_f}{\partial\mu_{Y_k}}\frac{\partial\mu_{Y_k}}{\partial\mu_{X_c}} + \frac{\partial P_f}{\partial\mu_{Y_\omega}}\frac{\partial\mu_{Y_\omega}}{\partial\mu_{X_c}} \\ \frac{\partial P_f}{\partial\mu_{X_k}} = \frac{\partial P_f}{\partial\mu_{Y_m}}\frac{\partial\mu_{Y_m}}{\partial\mu_{X_k}} + \frac{\partial P_f}{\partial\mu_{Y_c}}\frac{\partial\mu_{Y_c}}{\partial\mu_{X_k}} + \frac{\partial P_f}{\partial\mu_{Y_k}}\frac{\partial\mu_{Y_k}}{\partial\mu_{X_k}} + \frac{\partial P_f}{\partial\mu_{Y_\omega}}\frac{\partial\mu_{Y_\omega}}{\partial\mu_{X_k}} \\ \frac{\partial P_f}{\partial\mu_{X_\omega}} = \frac{\partial P_f}{\partial\mu_{Y_m}}\frac{\partial\mu_{Y_m}}{\partial\mu_{X_\omega}} + \frac{\partial P_f}{\partial\mu_{Y_c}}\frac{\partial\mu_{Y_c}}{\partial\mu_{X_\omega}} + \frac{\partial P_f}{\partial\mu_{Y_k}}\frac{\partial\mu_{Y_k}}{\partial\mu_{X_\omega}} + \frac{\partial P_f}{\partial\mu_{Y_\omega}}\frac{\partial\mu_{Y_\omega}}{\partial\mu_{X_\omega}} \end{cases} \tag{48}$$

Let $B = A^T$, the functional relationship between the mean value of the random variable under the Y coordinate and the X coordinate can be obtained as Eq. (49).

$$\mu_{Y_I} = \sum_{k=1}^{4} b_{ik}\mu_{X_k} \tag{49}$$

It is known that the partial derivatives of the reliability to the standard deviation of the random variables m, c, k and ω under the X coordinate can be expressed as Eq.(50).

$$\frac{\partial P_f}{\partial\sigma_{X_k}} = \sum_{i=1}^{4}\frac{\partial P_f}{\partial\sigma_{Y_I}}\frac{\partial\sigma_{Y_I}}{\partial\sigma_{X_k}} + \sum_{i=1}^{4}\sum_{j=1, j\neq i}^{4}\frac{\partial P_f}{\partial\rho_{Y_iY_j}}\frac{\partial\rho_{Y_iY_j}}{\partial\sigma_{X_k}} \tag{50}$$

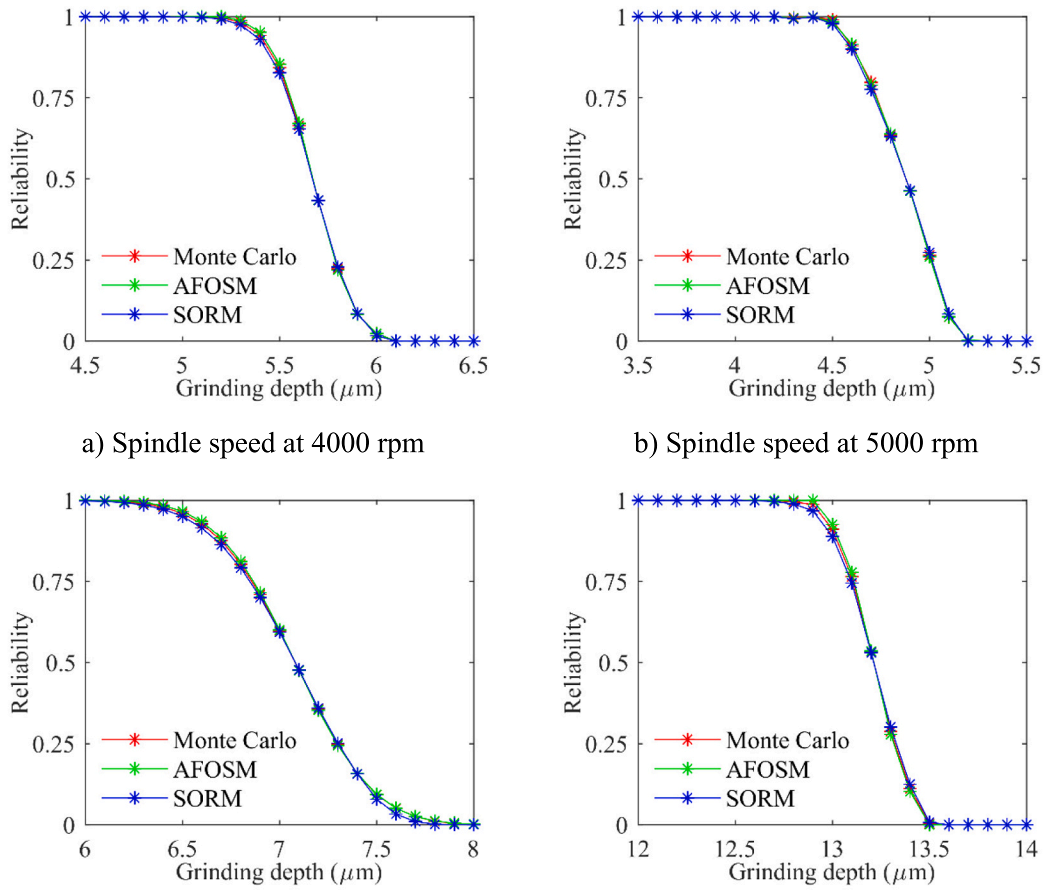

a) Spindle speed at 4000 rpm b) Spindle speed at 5000 rpm

c) Spindle speed at 5500 rpm d) Spindle speed at 6000 rpm

Fig. 7. Comparison of reliability results from different methods.

Expanding Eq. (46) to m, Eq. (51) can be obtained.

$$\frac{\partial P_f}{\partial \mu_{X_m}} = \frac{\partial P_f}{\partial \mu_{Y_m}}\frac{\partial \mu_{Y_m}}{\partial \mu_{X_m}} + \frac{\partial P_f}{\partial \mu_{Y_c}}\frac{\partial \mu_{Y_c}}{\partial \mu_{X_m}} + \frac{\partial P_f}{\partial \mu_{Y_k}}\frac{\partial \mu_{Y_k}}{\partial \mu_{X_m}} + \frac{\partial P_f}{\partial \mu_{Y_\omega}}\frac{\partial \mu_{Y_\omega}}{\partial \mu_{X_m}} + 2\left(\frac{\partial P_f}{\partial \mu_{Y_mY_c}}\frac{\partial \mu_{Y_mY_c}}{\partial \mu_{X_m}}\right.$$
$$\left. + \frac{\partial P_f}{\partial \mu_{Y_mY_k}}\frac{\partial \mu_{Y_mY_k}}{\partial \mu_{X_m}} + \frac{\partial P_f}{\partial \mu_{Y_mY_\omega}}\frac{\partial \mu_{Y_mY_\omega}}{\partial \mu_{X_m}} + \frac{\partial P_f}{\partial \mu_{Y_cY_k}}\frac{\partial \mu_{Y_cY_k}}{\partial \mu_{X_m}} + \frac{\partial P_f}{\partial \mu_{Y_cY_\omega}}\frac{\partial \mu_{Y_cY_\omega}}{\partial \mu_{X_m}} + \frac{\partial P_f}{\partial \mu_{Y_kY_\omega}}\frac{\partial \mu_{Y_kY_\omega}}{\partial \mu_{X_m}}\right) \tag{51}$$

Combined with Eq. (50), the function of the standard deviation under the Y coordinate and the X coordinate can be obtained as Eq. (52).

$$\sigma_{Y_l} = \sum_{k=1}^{4}\left(b_{ik}^2\sigma_{X_k}^2 + \sum_{k=1}^{4}\sum_{l=1,l\neq k}^{4} b_{jk}b_{jl}\rho_{X_kX_l}\sigma_{X_k}\sigma_{X_l}\right)^{\frac{1}{2}} \tag{52}$$

The partial derivative of the reliability with respect to the standard deviation of the random variables m, c, k and ω under the Y coordinate is $\partial\sigma_{Y_i}/\partial\sigma_{X_k}$, which expressed as Eqs. (53) and (54).

$$\rho_{X_iY_j} = \frac{1}{\sigma_{Y_i}\sigma_{Y_j}}\left(\sum_{k=1}^{4} b_{ik}b_{jk}\sigma_{X_k}^2 + \sum_{k=1}^{4}\sum_{l=1,l\neq k}^{4} b_{ik}b_{jl}\rho_{X_kX_l}\sigma_{X_k}\sigma_{X_l}\right) \tag{53}$$

$$\frac{\partial\rho_{X_iY_j}}{\partial\sigma_{X_k}} = \frac{1}{\sigma_{Y_i}\sigma_{Y_j}}\left(2\sum_{k=1}^{4} b_{ik}b_{jk}\sigma_{X_k} + 2\sum_{l=1,l\neq k}^{4} b_{ik}b_{jl}\rho_{X_kX_l}\sigma_{X_l}\right) \tag{54}$$

According to Eq. (52), the partial derivative $\partial\rho_{Y_iY_j}\rho/\partial\sigma_{X_k}$ with respect to m can be expanded as Eq. (55).

$$\frac{\partial\rho_{Y_mY_c}}{\partial\sigma_{X_m}} = \frac{2}{\sigma_{Y_m}\sigma_{Y_c}}\left(b_{11}b_{21}\sigma_{X_m} + b_{12}b_{22}\sigma_{X_c} + b_{13}b_{23}\sigma_{X_k} + b_{14}b_{24}\sigma_{X_\omega}\right.$$
$$\left. + b_{11}b_{22}\rho_{X_mX_c}\sigma_{X_c} + b_{11}b_{23}\rho_{X_mX_k}\sigma_{X_k} + b_{11}b_{24}\rho_{X_mX_\omega}\sigma_{X_\omega}\right) \tag{55}$$

where b_{ij} is the coefficient corresponding to matrix $B = A^T$.

Similarly, substituting the partial derivative of the reliability to the standard deviation of the random variable under the Y coordinate $\partial\sigma_{Y_i}/\partial\sigma_{X_k}$ and the functional relationship of the standard deviation under the Y coordinate and the X coordinate $\partial\sigma_{Y_i}/\partial\sigma_{X_k}$ into Eq. (49), the partial derivative of reliability against the standard deviations of the random variable m, c, k and ω the under the X coordinate can be obtained.

In order to study the influence of each random variable on the vibration response of the grinding system more accurately, the concepts of sensitivity gradient and sensitivity factor are introduced. It is known that the sensitivity gradient of the random variable X_k to the chatter of the grinding system under the X coordinate can be expressed as Eq. (56).

$$grad = \frac{\partial P_f}{\partial \mu_{X_k}}\vec{i} + \frac{\partial P_f}{\partial \sigma_{X_k}}\vec{j} \tag{56}$$

Then, the modulus of the gradient and the sensitivity factor can be obtained as Eqs. (57) and (58).

$$S_k = \sqrt{\left(\frac{\partial P_f}{\partial \mu_{X_k}}\right)^2 + \left(\frac{\partial P_f}{\partial \mu_{X_k}}\right)^2} \tag{57}$$

$$\lambda_k = \frac{S_k}{\sum_{i=1}^{4} S_i} \times 100 \ \% \tag{58}$$

Using the parameters of the cylindrical grinding system shown in Table 2, the sensitivity analysis can be carried out according to the above method, and the results are shown in Table 3. With the increase of the mean value of m, c and ω, the failure probability of the system will decrease, i.e., the grinding system is more stable and the system reliability is enhanced. As the mean value of k increases, the failure probability of the cylindrical grinding system will increase, i.e., the grinding system will be more unstable and the system reliability will decrease. With the increase of the mean square error of variables c, k and ω, the failure probability of the cylindrical grinding system will decrease, that is, the grinding system will be more stable and the system reliability will be enhanced.

The modulus and sensitivity factor of the calculated sensitive gradient are shown in Table 4. It can be observed that the modal mass m has the greatest influence on the reliability of the grinding system, and its sensitivity factor is up to 81.909 %. The rest factors are listed as k, c and ω, according to their influence on the grinding stability. Therefore, in order to ensure the stable grinding of the high-speed cylindrical machining system, special attention should be paid to the value of the modal mass to ensure that its variable range within a controllable range.

6. Experimental verification

The high speed cylindrical grinding experiments were carried out on a CNC camshaft grinder with model number CNC8325, the workpiece was a metal bar made of GCr15, and the grinding wheel was a CBN grinding wheel with primary structure made of Carbon Fiber Reinforced Plastics (CFRP). The water-based cooling method with a liquid supply pressure of 8 MPa is adopted along the grinding process. The experiment setup is shown in Fig. 8 and the used specific parameters are shown in Table 5.

According to the actual performance of the grinding machine and for better comparison, the grinding experiment was conducted at a given grinding depth with different spindle speeds 4000 rpm, 4500 rpm, 5000 rpm, 5600 rpm and 7000 rpm. Grinding chatter is identified through the vibration mark on the surface of the workpiece, as shown in Fig. 9a). 15 groups of grinding parameters are selected and the SLD is plotted, as shown in Fig. 9b). The simulation results are compared with the experimental results as shown in Table 6.

It can be observed that the simulation results are consistent with the experiment results in most of the working conditions. However, in working conditions 5 and 11, there is difference between the simulation result of SLD and the experiment result, as shown in bold in Table 6. For working condition 5, the simulation result of SLD of the grinding system at the mean value of the random parameter is a stable grinding state, and the calculated MCS reliability is 0.686773, which indicating that the system reliability is relatively low and the probability of chatter is high.

Table 2
Parameters of the grinding system.

Parameters	Mean value	Standard deviation	Distribution type
Modal mass, m	24.9 kg	0.1	Normal distribution
Modal damping, c	521 N·s/m	30	Normal distribution
Modal stiffness, k	3.07×10^6 N/m	1×10^5	Normal distribution
Chatter frequency, ω	985.2 rad/s	2.85	Normal distribution
Grinding depth, h	6.701×10^{-6} m	–	–
Spindle speed, Ω	5500 rpm	–	–

Table 3
Solutions for mean and standard deviation reliability sensitivity.

Mean sensitivity	$\partial P_f/\partial \mu_m$	$\partial P_f/\partial \mu_c$	$\partial P_f/\partial \mu_k$	$\partial P_f/\partial \mu_\omega$
Estimated value	−0.0427	−2.0426	7.7654	−0.0020

Standard deviation sensitivity	$\partial P_f/\partial \sigma_m$	$\partial P_f/\partial \sigma_c$	$\partial P_f/\partial \sigma_k$	$\partial P_f/\partial \sigma_\omega$
Estimated value	0.1503	0.0133	−0.0138	0.0071

Table 4
Sensitive gradient modulus and sensitivity factor in grinding system.

Sensitivity factor	Sensitive gradient modulus	Sensitivity factor
m	0.1562	81.909 %
c	0.0133	6.974 %
k	0.0138	7.236 %
ω	0.0074	3.880 %

The experiment result proved that chatter occurred. On the contrary, for working condition 11, the simulation result of the SLD at the mean value shows that there is no chatter, and the calculated MCS reliability is 0.465654, which indicating that the reliability of the system is relatively low and the probability of chatter is high. The experiment result also proved that chatter occurs. Furthermore, by taking the reliability value into consideration, it can be observed that simulation results are consistent with the experiment results and the grinding is stable when the reliability is over 0.956638. When the reliability is less than 0.083650, the simulation results are also consistent with the experiment results but the grinding is chatter. However, when the reliability is moderate like 0.686773 and 0.465654, there will be difference between simulation results and experiment results and the reliability of simulation results is weak. There should be a threshold value of reliability to judge the simulation results and that will be studied in the future work of our research. Considering that the threshold value of reliability may change with the variation of machining parameters and dynamics parameters of the machining system, the approach of adopting thresholds is convenient but inaccurate, and some intelligent algorithms based on experiment or experience are more promising.

The above analysis results show that there may be errors in the SLD under deterministic parameters under practical condition. The reliability research method with uncertain parameters proposed in this paper can evaluate the simulation results of the traditional SLD, thereby, improving the reliability of chatter prediction.

7. Conclusions

In order to avoid the damage caused by grinding chatter, the reliability of critical grinding depth considering the uncertain parameters in high speed cylindrical grinding is studied. The main conclusions are as follows:

(1) Based on the regenerative chatter mechanism, a single degree of freedom cylindrical grinding dynamic model was established. The uncertainty modeling and analysis of the grinding system were conducted by using the Monte Carlo method. The SLD with uncertain parameters was solved, and the distribution and mean value of the chatter frequency were solved by the numerical calculation.

(2) Considering the influence of random parameters on the grinding stability, an update of improved first-order second-moment method was proposed to analyze the chatter reliability. The reliability values of the grinding system were solved by using the Monte Carlo method, the improved first-order second-order moment method and the second-order second-order moment

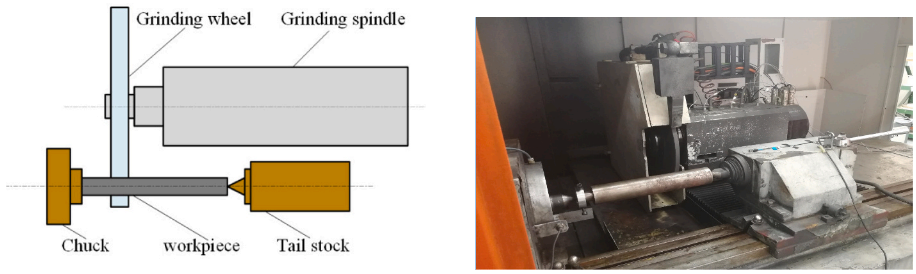

(a) Experimental block diagram (b) Experimental setup

Fig. 8. Grinding experiment.

Table 5
Parameters of grinding wheel, workpiece and grinding process.

Grinding wheel diameter	Grinding wheel thickness	Grinding wheel size	Workpiece length	Workpiece diameter	Spindle speed of grinding wheel	Cutting depth	Feed speed
0.5 m	0.0155 m	140	0.27 m	0.06 m	120 m/s	5×10^{-4} m	5×10^{-6} m/s

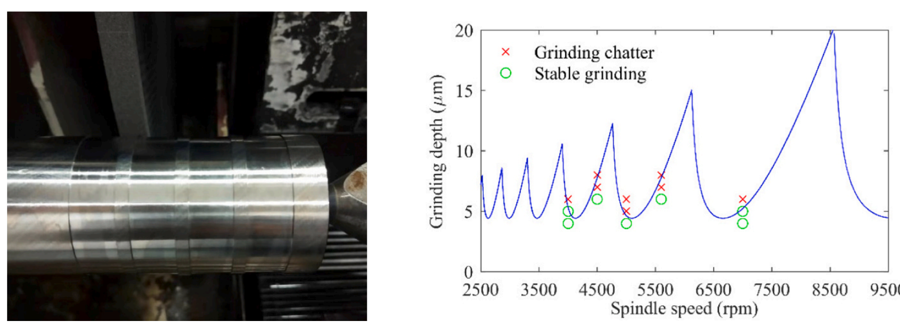

a) Vibration mark on workpiece surface b) Grinding stability lobe diagram

Fig. 9. Vibration mark and SLD of grinding system.

Table 6
Comparison of simulation and experiment results.

Number	Spindle speed (rpm)	Grinding depth (μm)	Simulated SLD results	Experiment results	Reliability
1	4000	4	Stable	Stable	1.000000
2		5	Stable	Stable	0.999012
3		6	Chatter	Chatter	0.023792
4	4500	6	Stable	Stable	1.000000
5		7	**Stable**	**Chatter**	0.686773
6		8	Chatter	Chatter	0.000000
7	5000	4	Stable	Stable	1.000000
8		5	Chatter	Chatter	0.265131
9		6	Chatter	Chatter	0.000000
10	5600	6	Stable	Stable	1.000000
11		7	**Stable**	**Chatter**	0.465654
12		8	Chatter	Chatter	0.083650
13	7000	4	Stable	Stable	1.000000
14		5	Stable	Stable	0.956638
15		6	Chatter	Chatter	0.000000

method, respectively. By comparison, the reliability values calculated by the improved first-order second-order moment method and the second-order second-order moment method are consistent with the Monte Carlo method, and it is simpler and faster by using the proposed moment method.

(3) By using the Monte Carlo sensitivity analysis method, the influence of relevant normal random parameters on the reliability of the grinding system is calculated, and the influence of each sensitivity factor on the reliability of the grinding system is obtained. Among them, the modal mass of the grinding system has the greatest influence on the reliability of the system, therefore, its variation range should be taken seriously.

(4) By taking the impact tests and grinding experiments, the mean value and standard deviation of the system modal parameters were obtained and the chatter was identified by analyzing the vibration mark on the workpiece surface. The results show that there may be errors in the prediction results of the SLD, and the accuracy of the prediction results can be improved by using the grinding chatter reliability analysis.

Declaration of competing interest

The authors declare that they have no known competing financial interests or personal relationships that could have appeared to influence the work reported in this paper.

Acknowledgements

This work was supported by the fund of Henan Key Laboratory of Superhard Abrasives and Grinding Equipment, Henan University of Technology [grant number JDKFJJ2022002]; the Key Scientific and Technological Project of Henan Province [grant number 232102220094]; and the National Natural Science Foundation of China [grant numbers 12072106, U2016054].

References

[1] Brinksmeier E, Mutlugünes Y, Klocke F, Aurich JC, Shore P, Ohmori H. Ultra-precision grinding. CIRP Ann Manuf Technol 2010;59(2):652–71. https://doi.org/10.1016/j.cirp.2010.05.001.

[2] Yang L, Chu CH, Fu YC, Xu JH, Liu YT. CFRP grinding wheels for high speed and ultra-high speed grinding: a review of current technologies and research strategies. Int J Precis Eng Man 2015;16:2599–606. https://doi.org/10.1007/s12541-015-0332-6.

[3] Inasaki I, Karpuschewski B, Lee HS. Grinding chatter — origin and suppression. CIRP Ann-Manuf Techn 2001;50(2):515–34. https://doi.org/10.1016/S0007-8506(07)62992-8.

[4] Munoa J, Beudaert X, Dombovari Z, Altintas Y, Budak E, Brecher C, et al. Chatter suppression techniques in metal cutting. CIRP Ann 2016;65(2):785–808. https://doi.org/10.1016/j.cirp.2016.06.004.

[5] Altintas Y, Stepan G, Budak E, Budak E, Schmitz T, Kilic ZM. Chatter stability of machining operations. J Manuf Sci Eng 2020;142(11). https://doi.org/10.1115/1.4047391.

[6] Wang WK, Wan M, Zhang WH, Yang Y. Chatter detection methods in the machining processes: a review. J Manuf Proc 2022;77:240–59. https://doi.org/10.1016/j.jmapro.2022.03.018.

[7] Hahn RS. Vibrations of flexible precision grinding spindles. J Manuf Sci Eng 1959;81(3):201–5. https://doi.org/10.1115/1.4008301.

[8] Snoeys R, Brown D. Dominating parameters in grinding wheel—and workpiece regenerative chatter. In: Advances in machine tool design and research 1969. Pergamon; 1970. p. 325–48. https://doi.org/10.1016/B978-0-08-015661-3.50025-4.

[9] Altintas Y, Weck M. Chatter stability of metal cutting and grinding. CIRP Ann 2004;53(2):619–42. https://doi.org/10.1016/S0007-8506(07)60032-8.

[10] Li H, Shin YC. A study on chatter boundaries of cylindrical plunge grinding with process condition-dependent dynamics. Int J Mach Tool Manuf 2007;47(10):1563–72. https://doi.org/10.1016/j.ijmachtools.2006.11.009.

[11] Liu Z, Payre G. Stability analysis of doubly regenerative cylindrical grinding process. J Sound Vib 2007;301(3–5):950–62. https://doi.org/10.1016/j.jsv.2006.10.041.

[12] Kim P, Jung J, Lee S, Seok J. Stability and bifurcation analyses of chatter vibrations in a nonlinear cylindrical traverse grinding process. J Sound Vib 2013;332(15):3879–96. https://doi.org/10.1016/j.jsv.2013.02.009.

[13] Yan Y, Xu J, Wiercigroch M. Regenerative and frictional chatter in plunge grinding. Nonlin Dyn 2016;86:283–307. https://doi.org/10.1007/s11071-016-2889-8.

[14] Leonesio M, Parenti P, Bianchi G. Frequency domain identification of grinding stiffness and damping. Mech Syst Signal Pr 2017;93:545–58. https://doi.org/10.1016/j.ymssp.2017.02.028.

[15] Chen Y, Chen X, Xu X, Yu G. Quantitative impacts of regenerative vibration and abrasive wheel eccentricity on surface grinding dynamic performance. Int J Adv Manuf Technol 2018;96:2271–83. https://doi.org/10.1007/s00170-018-1778-3.

[16] Tóth M, Sims ND, Curtis D. An alternative wheel regenerative mechanism in surface grinding: distributed grit dullness captured by specific energy waves. Mech Syst Signal Pr 2022;162:107964. https://doi.org/10.1016/j.ymssp.2021.107964.

[17] Quintana G, Ciurana J. Chatter in machining processes: a review. Int J Mach Tool Manuf 2011;51(5):363–76. https://doi.org/10.1016/j.ijmachtools.2011.01.001.

[18] Duncan GS, Kurdi Schmitz TL, Snyder JP. Uncertainty propagation for selected analytical milling stability limit analyses. North Am Manuf Res Conf 2006:17–24.

[19] Totis G. RCPM—a new method for robust chatter prediction in milling. Int J Mach Tool Manuf 2009;49(3–4):273–84. https://doi.org/10.1016/j.ijmachtools.2008.10.008.

[20] Totis G, Sortino M. Polynomial chaos-kriging approaches for an efficient probabilistic chatter prediction in milling. Int J Mach Tool Manuf 2020;157:103610. https://doi.org/10.1016/j.ijmachtools.2020.103610.

[21] Zhang X, Zhu L, Zhang D, Ding H, Xiong YL. Numerical robust optimization of spindle speed for milling process with uncertainties. Int J Mach Tool Manuf 2012;61:9–19. https://doi.org/10.1016/j.ijmachtools.2012.05.002.

[22] Graham E, Mehrpouya M, Nagamune R, Park SS. Robust prediction of chatter stability in micro milling comparing edge theorem and LMI. CIRP J Manuf Sci Technol 2014;7(1):29–39. https://doi.org/10.1016/j.cirpj.2013.09.002.

[23] Huang X, Hu M, Zhang Y, Lv C. Probabilistic analysis of chatter stability in turning. Int J Adv Manuf Technol 2016;87:3225–32. https://doi.org/10.1007/s00170-016-8672-7.

[24] Liu Y, Li T, Liu K, Zhang Y. Chatter reliability prediction of turning process system with uncertainties. Mech Syst Signal Pr 2016;66:232–47. https://doi.org/10.1016/j.ymssp.2015.06.030.

[25] Löser M, Otto A, Ihlenfeldt S, Radons G. Chatter prediction for uncertain parameters. Adv Manuf 2018;6:319–33. https://doi.org/10.1007/s40436-018-0230-0.

[26] Hajdu D, Insperger T, Stepan G. Robust stability analysis of machining operations. Int J Adv Manuf Technol 2017;88:45–54. https://doi.org/10.1007/s00170-016-8715-0.

[27] Hajdu D, Borgioli F, Michiels W, Insperger T, Stepan G. Robust stability of milling operations based on pseudospectral approach. Int J Mach Tool Manuf 2020;149:103516. https://doi.org/10.1016/j.ijmachtools.2019.103516.

[28] Li K, He S, Liu H, Mao X, Li B, Luo B. Bayesian uncertainty quantification and propagation for prediction of milling stability lobe. Mech Syst Signal Pr 2020;138:106532. https://doi.org/10.1016/j.ymssp.2019.106532.

[29] Ahmadi K. Bayesian updating of modal parameters for modeling chatter in turning. CIRP J Manuf Sci Technol 2022;38:724–36. https://doi.org/10.1016/j.cirpj.2022.06.006.

[30] Sun C, Niu Y, Liu Z, Wang Y, Xiu S. Study on the surface topography considering grinding chatter based on dynamics and reliability. Int J Adv Manuf Technol 2017;92:3273–86. https://doi.org/10.1007/s00170-017-0385-z.

[31] Liu T, Deng Z, Luo C, Lv L, Li Z, Wan L. Stability modeling and analysis of non-circular high-speed grinding with consideration of dynamic grinding depth. Chin J Mech Eng 2021;57(15):264–74 (in Chinese), https://doi.org/10.3901/JME.2021.15.264.